

**Copper- and silver-containing heterometallic iodobismuthates(III) with 4-(dimethylamino)-1-methylpyridinium cation: structures, thermal stability and optical properties**

**Irina A. Shentseva, Andrey N. Usoltsev, Pavel A. Abramov, Vladimir R. Shayapov, Nikita A. Korobeynikov, Maxim N. Sokolov and Sergey A. Adonin**

**Experimental section**

4-(dimethylamino)pyridine, BiI<sub>3</sub>, acetonitrile, acetone and ethanol were obtained from commercial sources and used without additional purification. 1-methyl-4-(dimethylamino)pyridinium iodide was prepared by the reaction of 4-(dimethylamino)pyridine with methyl iodide, the product was identified by <sup>1</sup>H NMR spectra and elemental analysis data.

**(1) (MeDMAP)<sub>2</sub>Bi<sub>2</sub>Cu<sub>2</sub>I<sub>10</sub>**

30 mg BiI<sub>3</sub> (0.05 mmol), 9.5 mg CuI (0.05 mmol) and 12 mg (0.05 mmol) 1-methyl-4-(dimethylamino)pyridinium iodide were dissolved in 5 ml of a mixture of solvents CH<sub>3</sub>CN/acetone (1:1) by heating to 70°C for 1 h. After dissolution, 5 ml of EtOH was added to the mixture. Then the solution was slowly cooled to room temperature and kept for 1 day. Dark red crystals were obtained. Product yield: 63 %. Elem anal. Calcd for C<sub>16</sub>H<sub>26</sub>N<sub>4</sub>Bi<sub>2</sub>Cu<sub>2</sub>I<sub>10</sub>, %: C 9.20; H 1.26; N 2.68; Found: C 9.25; H 1.31; N 2.72.

**(2) (MeDMAP)<sub>2</sub>Bi<sub>2</sub>Ag<sub>2</sub>I<sub>10</sub>**

15 mg BiI<sub>3</sub> (0.025 mmol), 6 mg AgI (0.025 mmol) and 6.5 mg (0.025 mmol) 1-methyl-4-(dimethylamino)pyridinium iodide were dissolved in 24 ml of a mixture of solvents CH<sub>3</sub>CN/acetone (1:1) by heating to 70°C for 1 h. After dissolution, the mixture was slowly cooled to room temperature and kept for 1 day. After partial evaporation, red crystals were obtained. Product yield: 69%. Elem anal. Calcd for C<sub>16</sub>H<sub>26</sub>N<sub>2</sub>Bi<sub>2</sub>Ag<sub>2</sub>I<sub>10</sub> C 8.82; H 1.20; N 2.57; Found: C 8.85; H 1.27; N 2.63.

**Powder X-ray diffractometry**

XRD analysis of polycrystalline samples was performed on Shimadzu XRD-7000 diffractometer (CuK-alpha radiation, Ni – filter, linear One Sight detector, 5 – 50° 2θ range, 0.0143° 2θ step, 2s per step). Samples were slightly ground with hexane in an agate mortar, and the resulting suspensions were deposited on the polished side of a standard quartz sample holder, and a smooth thin layer being formed after drying. Plotting of PXRD patterns (Figures 1S and 2S) and data treatment was performed using X'Pert Plus software.

**Thermogravimetric analyses (TGA)** were carried out on a TG 209 F1 Iris thermobalance (NETZSCH, Germany). The measurements were made in a helium flow in the temperature range

of 30–450°C using the heating rate of 10°C min<sup>-1</sup> the gas flow rate of 60 mL min<sup>-1</sup> and open Al crucibles.

**Diffuse reflectance spectra** were measured on an setup which consists of a Kolibri-2 spectrometer (VMK Optoelektronica, Russia), fiber optic cable QR-400-7 (Ocean Optics, USA), and deuterium–tungsten lamp AvaLight-DHS (Avantes, Netherlands) (see V.R. Shayapov et al., New J. Chem. 2019, 43(9), 3927). The reference of 100% reflectance was BaSO<sub>4</sub> powder. The spectra were recorded five times in the wavelength interval of 300-1000 nm and then averaged to reduce the random error. Kubelka-Munk function  $F(R)$  was calculated using diffuse reflectance spectra:

$$F(R) = \frac{(1 - R)^2}{2R}, \quad (1)$$

where  $R$  is a diffuse reflectance coefficient. The Kubelka-Munk function represents as  $k/s$  ratio where  $k$  is absorption coefficient and  $s$  is a scattering coefficient:

$$F(R) \sim \frac{k}{s} \quad (2).$$

Energy band gap  $E_g$  was determined by the Tauc method<sup>72</sup>. The dependence of the  $\sqrt{F(R) \times E}$  value (where  $E=1240/\lambda$  is photon energy) *versus*  $E$  for **1** and  $d[\ln(F(R) \times E)]/dE$  *versus*  $E$  was plotted. The energy band gap was obtained by extrapolation of the linear portion of the dependence to the intersection with the energy axis.

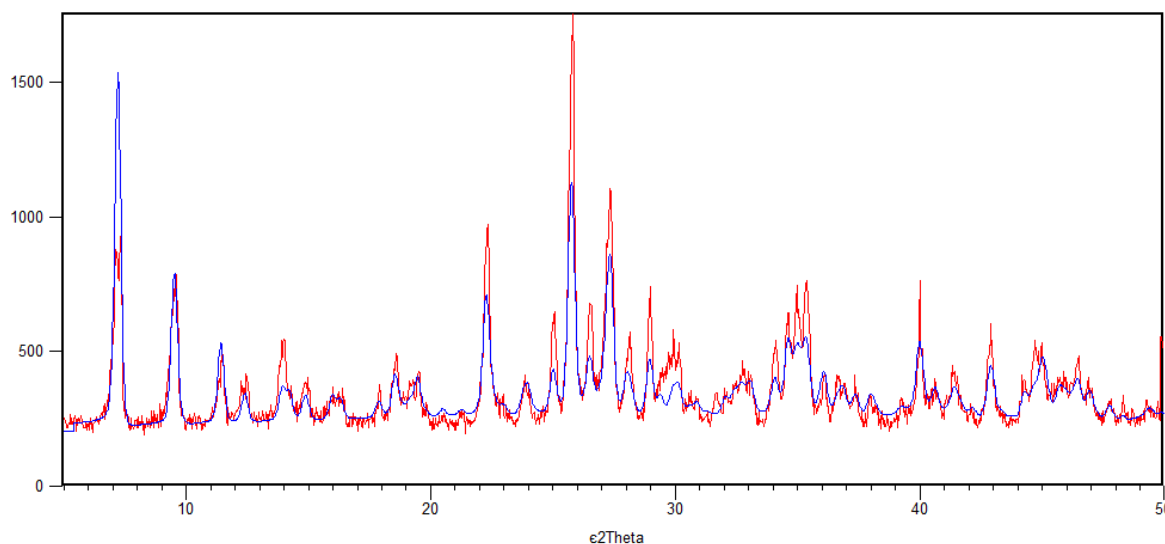


**Figure S1.** Calculated (blue) and experimental (red) PXRD patterns of **1**.

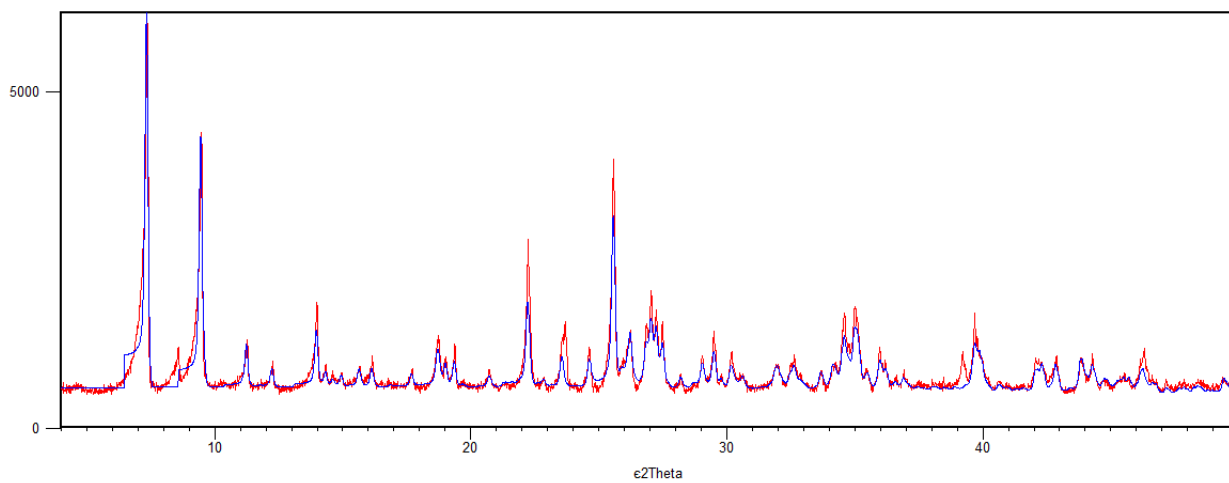


**Figure S2.** Calculated (blue) and experimental (red) PXRD patterns of **2**.